ChemPubSoc Europe

DOI: 10.1002/cbic.201402128

VIP

Computational Library Design for Increasing Haloalkane Dehalogenase Stability

Robert J. Floor,[a] Hein J. Wijma,[a] Dana I. Colpa,[a] Aline Ramos-Silva,[b] Peter A. Jekel,[a] Wiktor Szymański,[c] Ben L. Feringa,[c] Siewert J. Marrink,[d] and Dick B. Janssen*[a]

We explored the use of a computational design framework for the stabilization of the haloalkane dehalogenase LinB. Energy calculations, disulfide bond design, molecular dynamics simulations, and rational inspection of mutant structures predicted many stabilizing mutations. Screening of these in small mutant libraries led to the discovery of seventeen point mutations and one disulfide bond that enhanced thermostability. Mutations located in or contacting flexible regions of the protein had a larger stabilizing effect than mutations outside such regions. The combined introduction of twelve stabilizing mutations resulted in a LinB mutant with a 23 °C increase in apparent melting temperature ($T_{m,app}$, 72.5 °C) and an over 200-fold longer half-life at 60 °C. The most stable LinB variants also displayed increased compatibility with co-solvents, thus allowing substrate conversion and kinetic resolution at much higher concentrations than with the wild-type enzyme.

Introduction

Although enzymes are very proficient catalysts and can combine high acceleration of chemical reactions with good selectivity,[1] their application in industrial processes can be hampered by their limited stability.[2] For example, at high temperatures or in the presence of organic co-solvents, enzymes often lose activity due to unfolding and aggregation. Performing enzyme reactions at elevated temperatures has several benefits, such as improved solubility of reactants, higher conversion rates, and reduced risk of microbial contamination.[1–3] Improving intrinsic enzyme stability therefore contributes to the applicability of enzymes under realistic process conditions. Furthermore, thermostable enzymes are better suited than mesostable enzymes for improving catalytic activity by mutagenesis.[2c,4]

[a] R. J. Floor,[+] Dr. H. J. Wijma,[+] D. I. Colpa, P. A. Jekel, Prof. Dr. D. B. Janssen
Department of Biochemistry
Groningen Biomolecular Sciences and Biotechnology Institute
University of Groningen
Nijenborgh 4, 9747 AG Groningen (The Netherlands)
E-mail: d.b.janssen@rug.nl

[b] Dr. A. Ramos-Silva
Department of Biotechnology, Institute of Biomedical Sciences
University of Sao Paulo
Av. Prof. Lineu Prestes, 2415. Sao Paulo (Brazil)

[c] Dr. W. Szymański, Prof. Dr. B. L. Feringa
Center for Systems Chemistry, Stratingh Institute for Chemistry
University of Groningen
Nijenborgh 4, 9747 AG Groningen (The Netherlands)

[d] Prof. Dr. S. J. Marrink
Department of Biophysical Chemistry
Zernike Institute for Advanced Materials
University of Groningen
Nijenborgh 7, 9747 AG Groningen (The Netherlands)

[+] These authors contributed equally to this work.

Supporting information for this article is available on the WWW under http://dx.doi.org/10.1002/cbic.201402128.

Effective methods for improving intrinsic enzyme stability include directed evolution (repeated rounds of random mutagenesis and screening)[2b,5] and the introduction of consensus amino acids detected by multiple sequence alignments.[5b,6] Replacement of amino acids based on structural inspection and reconstruction of ancestral sequences have also been used.[2b,5] Directed evolution usually requires the screening of thousands of variants, and thus depends on high-throughput expression and assay methods, which are not always available. Rationally predicted stabilizing mutations can be found with less experimental screening effort and have also been used.[7] However, the design of individual stabilizing mutations is often complicated and time-consuming.[5c] Computational design has evolved from rational design and can predict many potentially stabilizing mutations based on free energy calculations, and can replace or complement chemical intuition. Computational methods led to an improvement in the apparent melting temperature ($T_{m,app}$) of small proteins of more than 15 °C,[8] while reducing the amount of experimental screening needed to identify stabilized variants.

Many approaches for the computational design of proteins with enhanced thermostability have been explored.[8c] One method is calculation of the electrostatic contributions of surface charges to the overall stability of the protein, and subsequent removal of charges that have destabilizing contributions. This method was used to improve the $T_{m,app}$ of an acylphosphatase and GTPase by 9 °C.[9] Another approach uses semi-empirical force fields to compute the differences in folding energy ($\Delta\Delta G^{fold}$) between the wild-type enzyme structure and the predicted mutant structures. Algorithms that can calculate such folding-energy differences include PoPMuSiC,[8e] FoldX,[8d,10] SCADES,[8a] and Rosetta.[11] RosettaDesign has been used to improve packing in the hydrophobic core of a protein, and this resulted in an 18 °C increase in melting temperature

of a domain of methionine aminopeptidase.[8b] Furthermore, the design of stabilizing disulfide bonds has been reported for several proteins.[12] However, computational methods to design chemically different types of stabilizing mutation in a single computational approach remain a challenge.[8c] It is also difficult to accurately predict the $\Delta\Delta G^{fold}$ required to achieve a large increase in unfolding temperature[8c] and to retain catalytic activity at low temperature in mutants with increased thermostability.[2c, 8a, 13]

We recently proposed a computational strategy for enzyme stabilization based on the calculation of folding energies for all possible substitutions, the integration of conformational sampling in disulfide-bond designs, and the use of molecular dynamics as a fast screening/ranking tool (FRESCO, framework for rapid enzyme stabilization by computation).[8f] The FRESCO strategy is not based on finding just a single or a few effective mutations, but on discovering and combining as many stabilizing mutations as possible—each of which might have only a small effect. Furthermore, as most of the screening is done in silico, the number of variants that needs to be produced and tested experimentally is significantly reduced. By using the FRESCO approach, the $T_{m,app}$ of limonene epoxide hydrolase was improved by 32 °C, with a total screening effort of less than 80 variants. The stabilization arose from both computationally designed point mutations and introduced disulfide bonds. The constructed enzymes, which contained 10–12 mutations, remained active at 30 °C.[8f]

In this study, we examined the use of FRESCO for the stabilization of a larger monomeric protein that catalyzes both the degradation of recalcitrant environmental pollutants and performs stereoselective biocatalysis,[14] that is, haloalkane dehalogenase (LinB, EC 3.8.1.5) from *Sphingomonas paucimobilis* UT26.[14b, 15] LinB is responsible for the hydrolytic dehalogenation of 1,3,4,6-tetrachloro-1,4-cyclohexadiene, which is an intermediate in the degradation pathway for the insecticide hexachlorocyclohexane (HCH, common name lindane).[15] It is also capable of hydrolysis of the highly recalcitrant β-isomer of HCH,[16] and is a versatile dehalogenase that converts many chloro-, bromo-, and iodoalkanes, haloamides, and haloesters.[14a] Other environmental chemicals that are substrates for LinB include 1,2-dibromoethane, 1-bromo-2-chloroethane, 3-chloro-2-methylpropene, and 1-bromopropane.[14a, b] Furthermore, the enzyme can be used for the enantioselective preparation of α-bromoamides[14c] and haloalcohols.[14d] Its catalytic mechanism has been studied in depth by structural,[17] mutational,[17b, 18] and quantum mechanical methods.[19] However, the possibilities to engineer and apply the enzyme are limited by its mediocre stability, as was found when performing mutagenesis experiments aimed to improve the enzyme selectivity for the enantioselective conversion of *N*-benzyl-2-bromohexanamide (unpublished results). The limited stability results in a low tolerance of organic co-solvents,[20] thus restricting the use of co-solvents to solubilize hydrophobic substrates.[14c] In this paper, we demonstrate that, by a combination of computational design and experimental screening, the FRESCO approach can drastically improve both the thermostability of the enzyme and its tolerance of co-solvents.

Results

Computational design of point mutations

Previously, the FRESCO computational framework was applied to improve the $T_{m,app}$ of the small dimeric protein limonene epoxide hydrolase by 32 °C.[8f] Here we investigated whether this framework, which aims to reduce experimental screening to a minimum, is also applicable for the stabilization of the larger monomeric haloalkane dehalogenase LinB. We compared the effects on stability and activity by mutations close to the active site to those by mutations away from the active site. In a previous study, several mutations close to the active site were found to stabilize the haloalkane dehalogenase DhaA,[21] but such mutations often result in reduced catalytic activity. For the stabilization of LinB, mutations were first introduced more than 9 Å from the docked substrate *tert*-butyl-2-(2-bromopropanamido)acetate. This afforded the substitution of 233 residues; 63 other residues were excluded because of their proximity to the active site (21% of the protein; Figure 1A, regions marked in red). Of the excluded residues, 35 were in six loops, and 28 were in three helices around the active site.

Subsequently, we used Rosetta[11b] and FoldX[10] to predict $\Delta\Delta G^{fold}$ in order to identify mutations which should stabilize LinB. Such point mutations can stabilize proteins by improving hydrophobic interactions in the interior, by removing unsatisfied hydrogen bonds, by improving surface electrostatic interactions, or by reducing the flexibility of areas that are rate-limiting for kinetic unfolding. FoldX predicted 150 possible stabilizing mutations, and Rosetta predicted 314 mutations with $\Delta\Delta G^{fold}$ higher than 3.5 kJ mol^{-1}. Of these, 57 were predicted by both methods, so a total of 407 unique stabilizing substitutions were expected. Previous work suggests that although FoldX and Rosetta can be used to find stabilizing mutations, these programs also give false-positive predictions.[8f, 13, 22] Therefore, the predicted structures of the mutants were visually inspected to eliminate mutants that harbored unconvincing substitutions (resulting from known problems in computational design), such as hydrophobic residues exposed at the surface, internal cavities, and missing hydrogen-bond interactions. The criteria for this elimination process are described in the Experimental Section. By this visual inspection, 219 variants were eliminated.

To reduce the required experimental screening effort, a further computational screening step by molecular dynamics simulations was performed. This procedure identifies unfavorable interactions that are not evident in the initial structure predicted by FoldX, but occur dynamically during MD simulations. Previous MD studies showed that several short parallel MD simulations can simulate an enzyme as well as one long simulation.[23] Therefore, five parallel MD simulations of 100 ps were performed for each mutant with varying initial atom velocities to obtain different samplings of conformational space. The MD screening eliminated 79 of the 188 variants. The majority of the mutations that were eliminated showed changes in the conformation of the introduced and surrounding residues during the simulation, compared to the structures predicted

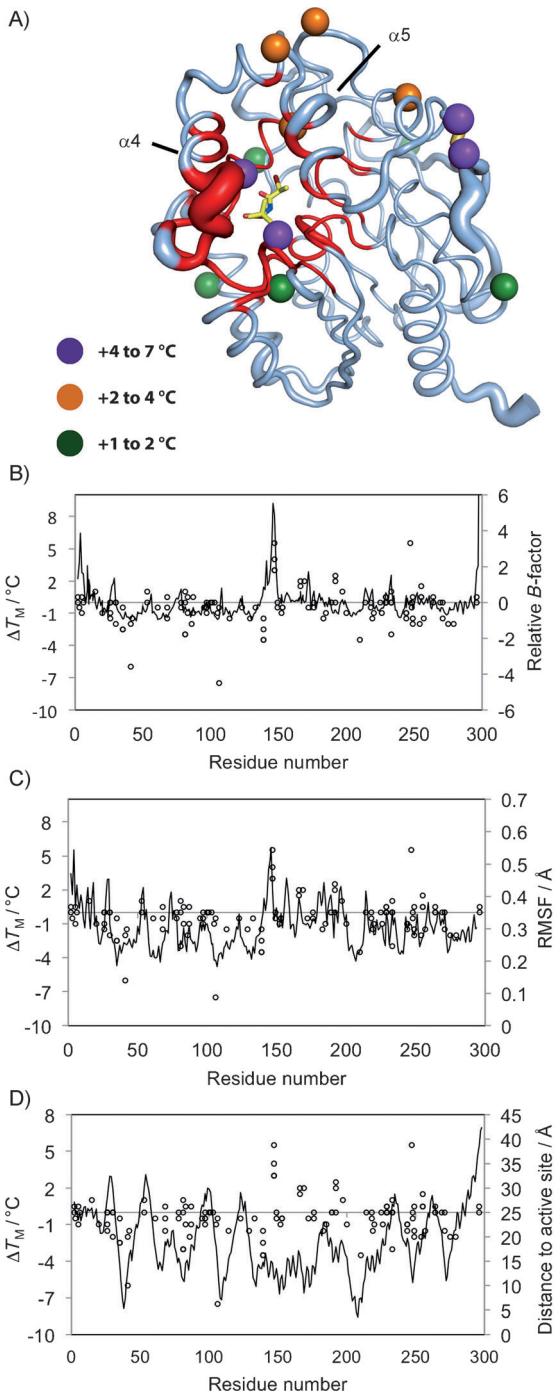

Figure 1. Correlation between flexibility and stabilizing effect of mutations in LinB. A) Sites of stabilizing mutations shown on the X-ray structure of LinB. Residues within 9 Å of the substrate *tert*-butyl-2-(2-bromopropanamido)acetate bound in the active site are shown in red. The thickness of the backbone represents the protein flexibility as determined by *B*-factor. Colored spheres indicate the effect of the mutation on $T_{m,app}$. The introduced disulfide bond (yellow) is between two purple spheres. Structure drawn from PDB ID: 1MJ5, with the docked substrate shown in sticks. B) Values for $\Delta T_{m,app}$ of the introduced mutations (○) and *B*-factors (——) against residue number. C) $\Delta T_{m,app}$ of the introduced mutations (○) and RMSF (——) against residue number. D) $\Delta T_{m,app}$ of the introduced mutations (○) and Cα distances to the chloride ion bound in the active site (——) against residue number.

by FoldX. This resulted in unsatisfied hydrogen bonds, the removal of α-helix-capping interactions, or the breaking of a salt bridge. Finally, 109 designed mutations that passed the MD screening were selected for experimental analysis.

Mutants were constructed by QuikChange reactions in microtiter plates (MTPs). Subsequently, cells producing the protein of interest were grown in MTP plates and, after lysis, the enzymes were purified by affinity chromatography. With this procedure, soluble protein was obtained from *Escherichia coli* cells for 99 of the 109 mutants (Table S1 in the Supporting Information). To verify the predicted stabilizing effects of these mutations, mutant $T_{m,app}$ values were experimentally determined by using the thermofluor method.[24] $T_{m,app}$ does not correlate directly with $\Delta\Delta G^{fold}$, which was used for the computational prediction, but earlier research suggested that $T_{m,app}$ correlates well with enzyme half-life and activity at higher temperature.[8f,25] The use of $T_{m,app}$ was preferred instead of the more commonly used quantification of the residual activity after heating the enzyme, as the latter can be influenced by variations in protein refolding, instead of improvements in intrinsic stability.[26]

The obtained $T_{m,app}$ values were compared to the melting temperature of the wild type to obtain $\Delta T_{m,app}$. Mutations that gave a $\Delta T_{m,app}$ at least twofold higher than the standard deviation of the assay (±0.96 °C, $n=9$) were scored as stabilizing. This resulted in the discovery of ten stabilizing mutations (Table 1), a success rate of 10% (number of mutations experimentally found to be stabilizing divided by the number of predicted mutations, Table S1). Different types of stabilizing mutations were experimentally observed (Table 1 and Figure 2): introduction of a proline into a loop (A197P), removal of negative charge from the surface (E15T, D166N, and D255A), introduction of a positive surface charge (A81K, D166K, E192K, and E192R), improving hydrophobic packing in the interior of the protein (A53L), and replacing a glycine in a loop (G229Q).

To determine if the discovered stabilizing mutations affected dehalogenase activity, specific activities of the purified enzymes were determined with 1-bromopropane. Nearly all variants were as active as the wild-type enzyme (Table 1), thus supporting the expectation that mutations stabilizing LinB away from the active site do not reduce its activity.

The majority of the tested mutations had neither a significantly positive nor a significantly negative effect on stability (56% of the mutations, Table S2). This suggests that most of the $\Delta\Delta G^{fold}$ differences of the mutations do not significantly influence the overall stability of the protein. Possibly, a labile region of the protein (one not influenced by the expected stabilizing mutations) determines the overall unfolding.[7b,27]

Design of disulfide bonds

The DDD algorithm[8f] was used to predict suitable locations for the introduction of disulfide bonds, based on both the geometry of the S–S bond and the molecular mechanics energy. Disulfide bonds are known to stabilize proteins both thermodynamically (reducing the entropy of the unfolded state) and kinetically (slowing important steps in protein unfolding path-

Table 1. Stabilizing mutations in LinB.

Parent	Origin	$\Delta\Delta G^{fold}$ [kJ mol^{-1}]	Mutation(s)	$T_{m,app}$ [°C]	$\Delta T_{m,app}$ [°C]	Relative activity[b]
LinB WT variants						
wild-type			–	51.0	0.0	±
wild-type	Rosetta	−4.2	E15T	52.0	1.0	±
wild-type	Rosetta	−4.0	A53L	52.0	1.0	–
wild-type	Rosetta	−4.0	A81K	52.0	1.0	±
wild-type	Rosetta	−9.2	D166K	53.5	2.5	+
wild-type	Rosetta	−4.3	D166N	53.0	2.0	n.d.
wild-type	FoldX	−3.7	E192K	54.0	3.0	±
wild-type	FoldX	−4.6	E192R	53.5	2.5	n.d.
wild-type	FoldX	−4.0	A197P	52.5	1.5	+
wild-type	–	–	G229Q + E192R[a]	54.0	3.9	+
wild-type	Rosetta	−5.0	D255A	51.5	0.5	±
wild-type	DDD/MD	–	A5C/A185C	56.0	5.0	±
wild-type	variant G1		A5C + A185C + G229Q + D166K + E192K	62.0	11	±
LinB G1 variants						
G1	Rosetta	−15.9	D147H	65.0	3.0	– –
G1	Rosetta	−25.4	D147Y	67.5	5.5	– – –
G1	Rosetta	−9.2	D147M	65.0	3.0	– – –
G1	Rosetta	−15.8	D147L	66.0	4.0	– – – –
G1	Rosetta	−5.8	F169V	64.0	2.0	+
G1	FoldX	−5.8	T249L	62.5	0.5	±
G1	FoldX	−4.0	A247F	67.5	5.5	– – –
G1	variant G3	–	E15T + A53L + A81K + F169V + A197P + D255A + A247F	74.0	12, 23[c]	– –

[a] $T_{m,app}$ determined for the double mutant. E192R occurred by accident. [b] Symbols: –: activity with 1-bromopropane reduced by 10–25%; – –: reduced by 25–50%; – – –: reduced by 50–75%; – – – –: reduced by 75–100%, ±: similar to wild type; +: improved by 10–25%; n.d.: not determined. [c] Compared to variant G1 and wild type, respectively.

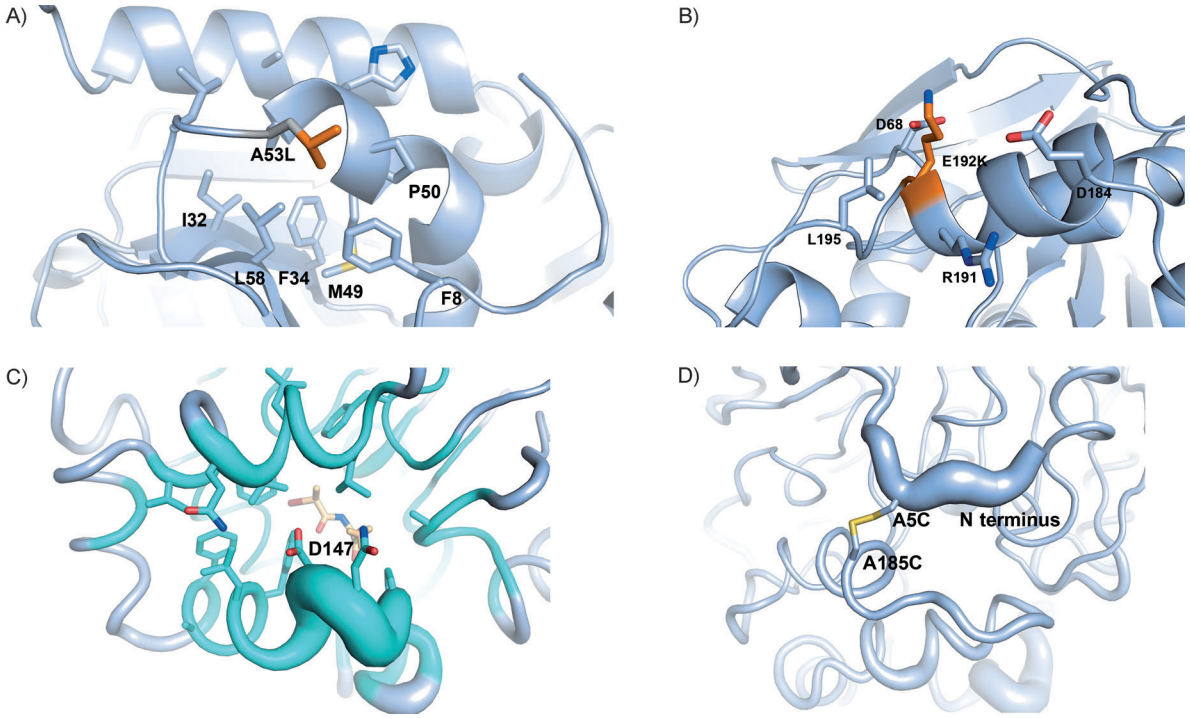

Figure 2. Structures of stabilized mutants as predicted by FoldX. A) Mutation A53L ($\Delta T_{m,app} = +1\,^{\circ}C$); structural inspection revealed that this mutation improves van der Waals interactions. B) Mutation E192K ($\Delta T_m = +3\,^{\circ}C$); the introduced lysine (orange) resulted a positive charge at the surface. In the predicted structure, K192 has only long-range electrostatic interactions (>7.5 Å). C) Model based on the structure of wild-type LinB (PDB ID: 1MJ5) highlighting residue D147, which is located in a flexible loop near the active site. Mutation of D147 to H, Y, M, or L ($\Delta T_m = +3.0$–$5.5\,^{\circ}C$) improves stability but reduces activity. The docked substrate *tert*-butyl-2-(2-bromopropanamido)-acetate is shown in yellow to highlight its proximity to D147. D) Predicted structure with the disulfide bond introduced between residues 185 (protein core) and 5 (close to the N terminus); $\Delta T_m = +5\,^{\circ}C$. The flexibility of the wild-type protein, as observed by crystallographic *B*-factors, is represented by the thickness of the chain (3–35 Å^2) in panels C and D.

ways, such as local unfolding of flexible areas).[12a,b,28] Seven suitable residue pairs were predicted for the introduction of disulfide bonds, based on the X-ray structure (PDB ID: 1MJ5). To examine whether a larger number of disulfide bonds is possible, not only the X-ray structure but also snapshots of MD simulations were used to predict pairs of positions where disulfide-forming cysteines could be introduced. Previous experiments suggested that small variations in the positions of backbone atoms can have a large effect on the distances, angles, and dihedrals of the designed disulfide bonds, and therefore on the predicted molecular-mechanics energy of disulfide bonds.[8f] By using a set of MD-generated template structures for the predictions, an additional 25 pairs of cysteine positions were discovered, thus raising the total number of predicted pairs to 32.

After visual inspection of the mutants (based on criteria described in the Experimental Section) the dynamic behaviors of mutants carrying the predicted disulfide bonds were analyzed by MD simulations, in order to identify mutants with destabilizing features, such as surface-exposed aromatic residues or broken salt bridges. This analysis revealed that 19 of the 32 predicted disulfide bond mutations likely were destabilizing, and therefore they were eliminated.

The remaining 13 disulfide bond designs were characterized experimentally, with enzymes produced in both *E. coli* TOP10 and *E. coli* SHuffle (Table S3). The latter is optimized for the cytosolic formation of disulfide bonds.[29] This analysis revealed that only one of the 13 tested mutants was more stable. It carried a disulfide bond between residues 5 and 185, and this stabilized the protein by 5 °C (Table 1, Figures 1 and 2). The mutation was only stabilizing in its oxidized state (Table S3), thus indicating that the observed increase in $T_{m,app}$ can be attributed to the introduced disulfide bond. The dehalogenation activity of the stabilized variant A5C/A185C with the model substrate 1-bromopropane was similar to the wild-type activity (Table 1), thus indicating that the stabilizing disulfide bond does not diminish activity. This stabilizing disulfide bond was predicted by methods based on both the X-ray structure and structures generated by MD simulations.

Previously, a similar approach aimed at enhancing the stabilization of limonene epoxide hydrolase yielded thirteen stabilizing disulfide bonds.[8f] Other computational design studies have found one[12b–d] or two stabilizing disulfide bonds.[12a] For LinB, only one disulfide bond was found, and this yielded moderate stabilization. Possibly, local kinetic stabilization arising from the other examined disulfide bonds did not contribute to the overall stability of the protein. The stabilizing A5C/A185C disulfide bond was in the flexible N terminus of the protein (Figures 1 and 2); no stabilizing disulfide bonds were discovered at more rigid parts of the protein. The observed stabilization in a flexible area is consistent with results for other proteins.[12a,30]

To analyze why the other disulfide bonds were not stabilizing, the melting temperatures of all 13 disulfide-bond variants were determined in both the reduced and oxidized states. Six of these did not show a clear melting transition in their oxidized state (suggesting misfolding), whereas such a transition was seen when reduced (Table S3). This reduction resulted in proteins with clearly defined melting temperatures, thus indicating homogenous structures. These results suggest that unintended disulfide bonds were formed between the introduced and endogenous cysteine residues, as six of the 13 constructed disulfide bonds resulted in misfolded protein (Table S3).

Combining stabilizing mutations

To investigate whether a highly thermostable variant could be obtained by combining confirmed stabilizing mutations, we constructed mutant LinB-G1, in which three stabilizing point mutations (G229Q, D166K, and E192K) and one disulfide bond (A5C/A185C) were combined. The $T_{m,app}$ of this variant was 11 °C higher than that of the wild-type enzyme (Table 1, Figure 3 A and B). Its activity was preserved, with slightly higher

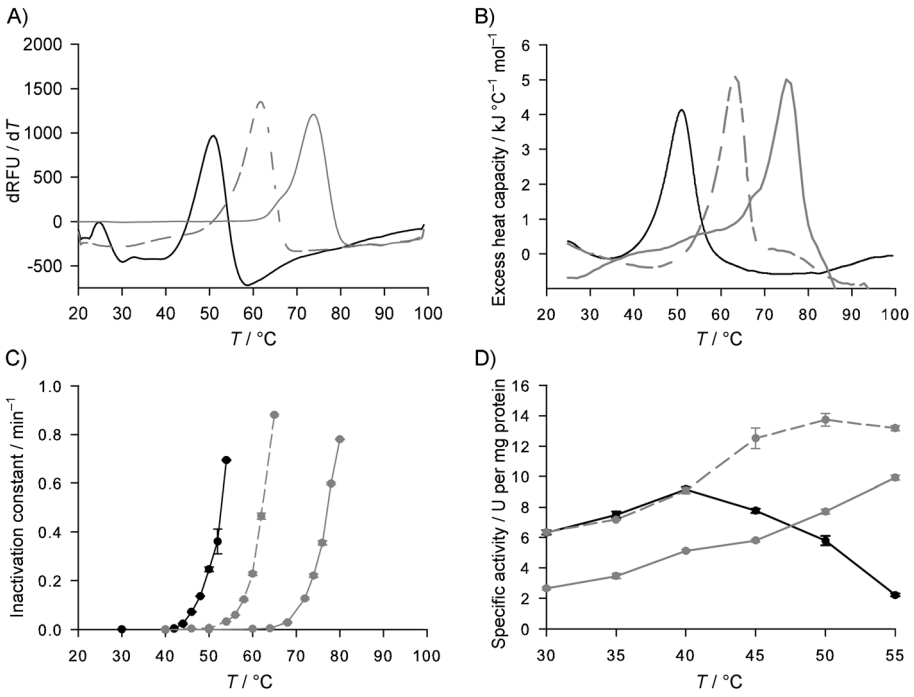

Figure 3. Thermostabilities of wild-type LinB and variants G1 and G3 determined by four different methods: wild type (black line), G1 (dashed line), G3 (gray line). A) $T_{m,app}$ measured (in the absence of cosolvent) by the thermofluor method. B) $T_{m,app}$ measured by DSC. C) Thermal inactivation constants at different temperatures. D) Specific activities for dehalogenation of 1-bromopropane at different temperatures. Because of the experimental setup, activities could only be measured up to 55 °C.

Table 2. Kinetics parameters for the dehalogenation of 1-bromopropane by wild-type LinB and variants G1 and G3 at 30 °C and at their optimum temperatures.

	30 °C			Optimum temperature			
Variant	k_{cat} [s^{-1}]	K_m [mM]	k_{cat}/K_m [s^{-1} mM^{-1}]	k_{cat} [s^{-1}]	K_m [mM]	k_{cat}/K_m [s^{-1} mM^{-1}]	T [°C]
wild-type	4.5 ± 0.2	1.9 ± 0.1	2.3	6.1 ± 0.3	3.2 ± 0.3	1.9	40
G1	4.7 ± 0.4	3.0 ± 0.2	1.6	6.7 ± 0.4	3.7 ± 0.1	1.8	50
G3	2.4 ± 0.1	1.3 ± 0.1	1.9	4.3 ± 0.6	2.4 ± 0.2	1.8	50

Table 3. Specific activities at 30 °C for the dehalogenation of several haloalkanes by wild-type LinB and variants G1 and G3.

	Wild-type LinB [U mg^{-1}]	LinB-G1 [U mg^{-1}]	LinB-G3 [U mg^{-1}]
Bromoalkanes			
1-bromohexane	1.2 ± 0.1	1.3 ± 0.2	0.8 ± 0.1
1-bromocyclohexane	1.5 ± 0.1	1.3 ± 0.1	1.5 ± 0.1
1-bromopropanen	6.3 ± 0.1	6.3 ± 0.1	2.7 ± 0.1
1,2-dibromomethane	7.1 ± 0.6	8.1 ± 0.6	0.5 ± 0.1
Chloroalkanes			
1-chloropropane	14 ± 0.3	12.2 ± 0.4	1.3 ± 0.1
1-chloroheptane	1.7 ± 0.1	1.8 ± 0.1	0.1 ± 0.05
1-chloropentane	1.5 ± 0.2	1.4 ± 0.1	0.9 ± 0.1
1-chlorobutane	1.3 ± 0.1	1.1 ± 0.1	1.2 ± 0.1
1,3-dichloropropane	0.9 ± 0.1	0.7 ± 0.1	0.3 ± 0.1
1-chlorocyclohexane	0.2 ± 0.1	0.1 ± 0.05	0.2 ± 0.1
Iodoalkanes			
1-iodopropane	4.7 ± 0.1	4.0 ± 0.1	2.7 ± 0.3

k_{cat} and higher K_m for the dehalogenation of 1-bromopropane (Table 2). The dehalogenase activities for a range of other haloalkanes and halocycloalkanes were also found to be almost the same as for the wild type (Table 3). This supports the hypothesis that stabilizing mutations away from the active site do not affect activity, and indicates that the mutations did not indirectly disturb the active site or parts of the enzyme that need to be flexible for substrate access or product release. The observed increase in K_m suggests[14c] that, due to the mutations, either an early step in the catalytic mechanism had become slower than the later reactions steps or that the mutations slightly reduced substrate binding.

The correlation between increased $T_{m,app}$ and protein unfolding and activity at elevated temperatures was investigated by measuring inactivation rates and enzyme activity at higher temperatures. The rate of unfolding of variant G1 was significantly lower than that of the wild type (increased half-lives at elevated temperatures: 40-fold at 50 °C and 20-fold at 54 °C, Figure 3C). The activities of both wild type and G1 increased with temperature, but the wild-type enzyme reached optimum activity at 40 °C, whereas G1 showed its highest activity at 50 °C. At the optimum temperatures, G1 was 1.5-fold more active than wild type (Figure 3D). Thus, the 11 °C improvement in the $T_{m,app}$ of variant G1 (Figure 3A and B) reflects significantly improved half-life and activity at and above 44 °C.

Mutations close to the active site

It has been suggested that stabilization of flexible areas of a protein contributes more to the overall stability than does stabilization of rigid areas.[7b,27,31] For LinB, the region surrounding the active site is relatively flexible (Figure 1). Structural inspection and analysis of the *B*-factors of the protein revealed that the most flexible parts of two helixes (α4, residues 144–148, and α5, 169–173) flank the active site (Figure 1B). The crystallographic *B*-factors of this area are 1.5-fold higher than the average for the protein (9.1 and 5.6 $Å^2$, respectively). Furthermore, the root-mean square fluctuation (RMSF) calculated from MD simulations of the wild-type enzyme was 1.5-fold higher in helix α4 (residues 144–148). Indeed, with the exception of the N and C termini, helix α4 is the most flexible part of the protein, based on *B*-factor and RMSF (Figure 1B and C). The active site of LinB is buried in the protein, and substrates reach it through an access tunnel. It was reported that flexibility of residues lining this tunnel (169–173) is required for substrate access to the active site.[32] Therefore, this area could be an interesting region for the introduction of stabilizing mutations, although this bears the risk of incurring a negative effect on catalytic activity.

To investigate whether mutations close to the active site (< 9 Å from the bound chloride) have a larger effect on overall stability, potentially stabilizing mutations were computationally designed by the above approach, including folding-energy predictions, structural inspection, and MD simulations. This predicted 27 stabilizing mutations. These were constructed by QuikChange mutagenesis in a LinB-G1 background; 24 mutants were successfully produced, and their $T_{m,app}$ values were measured by the thermofluor assay. This resulted in the discovery of seven additional stabilizing mutations (Table 1). The success rate for mutations introduced close to the active site (29%) was much higher than for mutations distant from the active site (10%). Five of the seven stabilizing mutations improved packing of hydrophobic residues in the apolar interior of the protein close to the active site (D147M, D147L, F169V, A247F, T249L, Figure 2C). Residues 247 and 249 are in a loop covering the active site and interact with a flexible helix (residues 139–156). Residue 147 is at the beginning of a very flexible stretch of this helix. All mutations that replaced this residue with a less polar amino acid stabilized the enzyme significantly (Table 1). Likely, the residue at this position influences the flexibility of the two most flexible residues of the active site, E145 and N146.

Stabilizing mutations close to the active site had a more pronounced effect on overall thermostability. For mutations near

the active site, 66% (16 of 24) affected overall stability, whereas only 44% of distal mutations (44 of 99 variants characterized) influenced stability, even though the design procedures were very similar (Table S1). Mutations that improved local folding interactions (e.g., by optimizing packing in the hydrophobic interior) were much more stabilizing when close to the active site (4 of 13, compared to 2 of 34). Away from the active site, seven out of ten mutations stabilized the enzyme by improving long-range electrostatics at the surface. This suggests that mutations that improve local folding interactions close to the active site contribute more to the overall stability of LinB.

Assays were carried out with 1-bromopropane to analyze whether stabilizing mutations close to the active site influence activity: five of the seven stabilizing mutations significantly reduced the activity of the enzyme; only mutations F169V and T249L increased stability while retaining activity (Table 1). Thus, although 29% of the mutations surrounding the active site were stabilizing (compared with 10% for those outside this area), most (71%) diminished activity, whereas all but one of the more distant mutations retained catalytic activity.

Combining mutations to obtain a further stabilized variant

It was investigated whether it is possible to obtain a hyperstabilized variant by combining all the moderately and highly stabilizing mutations. Thus, stabilizing mutations E15T/A53L/A81K/A197P/D255A (distant from the active site) and F169V/A247F (close to the active site) were introduced into variant G1. The resulting variant (LinB-G3) contained ten stabilizing point mutations and one disulfide bond. Its $T_{m,app}$ was measured by both differential scanning calorimetry (DSC) and thermofluor assays: $T_{m,app}$ was $(74 \pm 0.5)^{\circ}C$, an increase of $23^{\circ}C$ over wild type (Figure 3A and B). This resulted in improvements to other parameters relevant for biocatalysis, such as half-life and activity at higher temperatures: half-life was 200 min at $60^{\circ}C$, compared to just 1.0 min at $55^{\circ}C$ for the wild type (Figure 3C).

To determine activity, variant G3 was assayed with 1-bromopropane and several other chloroalkanes, iodoalkanes, and bromoalkanes (Table 3). Most of the G3 mutations did not reduce enzymatic activity individually (Table 1). However, activity at $30^{\circ}C$ was reduced when the mutations were combined: k_{cat} for 1-bromopropane was reduced (46%), K_m was also weaker (1.9 vs. 1.3 mM), and there was a moderate reduction (19%) in catalytic efficiency (k_{cat}/K_m, Table 2). The activity for several other haloalkanes was also lower (Table 3). However, the improved thermal stability allowed variant G3 to perform dehalogenation reactions at $55^{\circ}C$, whereas the wild-type enzyme starts to unfold above $40^{\circ}C$. Variant G3 is as active at its optimum temperature of $55^{\circ}C$ as the wild type at its optimum temperature of $40^{\circ}C$ (Figure 3D).

Improved degradation of β-hexachlorocyclohexane in DMSO/water

Thermostable enzymes often tolerate higher concentrations of co-solvent better than mesostable enzymes.[6c,21,33] This is advantageous for the conversion of poorly soluble substrates in water/co-solvent mixtures. To investigate whether the higher stabilities of the LinB variants were accompanied by higher tolerance of co-solvent, catalytic activity was determined in buffer containing 50% (*v/v*) DMSO or 1,4-dioxane (Figure 4A and B). $T_{m,app}$ values in the presence of DMSO or 1,4-dioxane were also determined. G1 and G3 were inactivated much more slowly, while their $T_{m,app}$ values in the presence of co-solvents were significantly increased over that of wild type (Figure 4C and D). G3 displayed some heterogeneity: a fraction of the enzyme initially unfolded but the rest of the protein retained activity over time (Figure 4B). These results clearly demonstrate that these thermostable variants are able to function significantly better in the presence of these co-solvents.

A unique property of LinB is its activity with the highly recalcitrant β-isomer of HCH.[16] However, efficient conversion by LinB is hampered by the poor solubility of this compound.[21] In water β-HCH is soluble up to only 17 μM,[16,21] but higher concentrations can be obtained in a DMSO/water mixture. To further improve the solubility of and activity towards β-HCH, the temperature was raised to $45^{\circ}C$. Activity assays with a tenfold higher concentration of β-HCH (180 μM in a DMSO/buffer mixture) at $45^{\circ}C$ showed superior conversion compared to that in buffer alone (Figure 5). Degradation of β-HCH by the wild-type enzyme and variant G1 in 25% DMSO at $45^{\circ}C$ was compared: G1 fully converted 180 μM β-HCH within 8 h (99% conversion), whereas the wild-type enzyme converted only 26% and was inactivated within 30 min (Figure 5). The concurrent increase in thermostability and solvent tolerance suggests that it is possible to enhance the performance of enzymes in organic solvents by engineering their stability.[6c,21,33]

To investigate the cause of the improved tolerance to co-solvent, $T_{m,app}$ was investigated in the presence of solvent. These experiments showed that reduced $T_{m,app}$ as a function of co-solvent concentration was rather similar for wild-type and G1 and G3 enzymes (Figure 4C and D). However, the higher melting temperatures of the thermostable variants without co-solvents resulted in higher $T_{m,app}$ values in the presence of co-solvent, even though the melting temperatures were lower for both the wild-type and mutant enzymes in the presence of co-solvent (Figure 4C and D). When the addition of co-solvent resulted in melting temperatures close to ambient temperature, LinB unfolded rapidly, as was the case for the wild-type enzyme in 25% 1,4-dioxane (Figures 3C and 4B). This demonstrates that the higher overall stability resulted in a higher $T_{m,app}$ and slower unfolding in the presence of co-solvent.

Kinetic resolution

In order to investigated whether the FRESCO method could improve the solvent tolerance of LinB while retaining enantioselectivity, variant G1 was used for the kinetic resolution of *tert*-butyl-2-(2-bromopropanamido)-acetate in the presence of co-solvent. LinB is highly enantioselective in this conversion, but the compound is soluble in water up to only 1500 μM.[14c] Variant G1 was used as it was the most promising mutant. Its

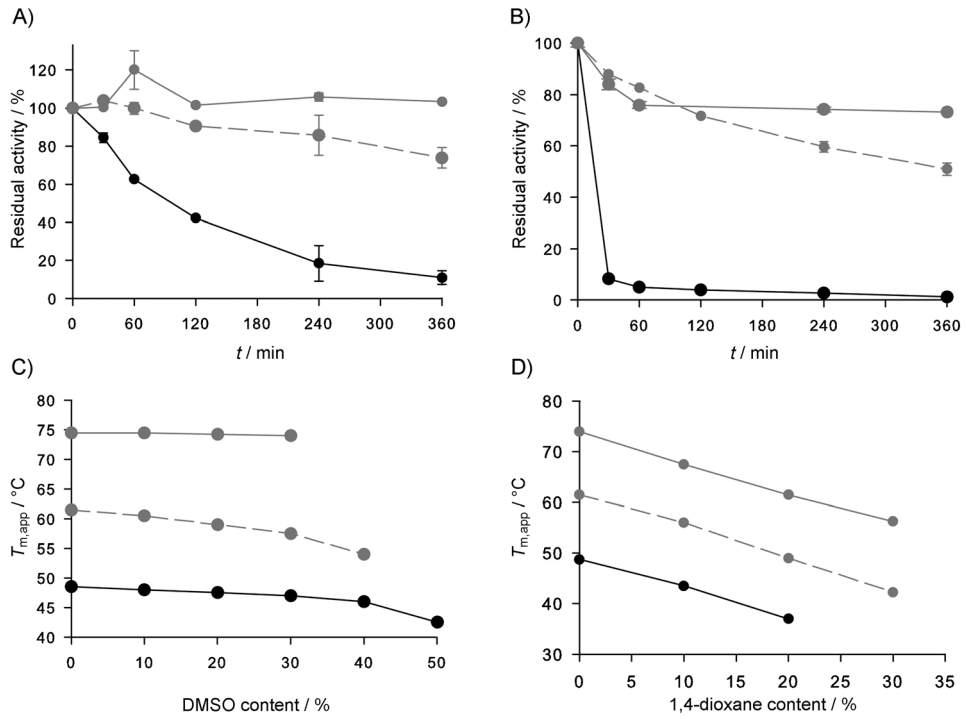

Figure 4. Comparison of activities and apparent melting temperatures of wild-type LinB (black line) and variants G1 (dashed line) and G3 (gray line) in buffer with organic co-solvent. A) Effect of the incubation time on the activity for the dehalogenation of 1-bromopropane in the presence of 50% DMSO. The initial activity without co-solvent was set to 100%. B) As above with 25% co-solvent 1,4-dioxane. C) Observed $T_{m,app}$ of the different variants in the presence of different amounts of DMSO. D) As above with 1,4-dioxane.

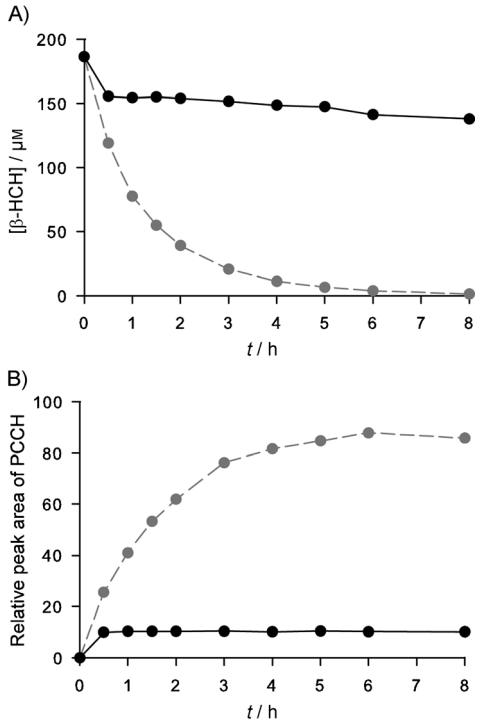

Figure 5. Conversion of 180 μM β-HCH by wild-type LinB (black line) and variant G1 (dashed line) at 45 °C in the presence of 25% DMSO (co-solvent). A) β-HCH concentration against time. B) Concentration of the product pentachlorocyclohexanol against time, as determined by relative GC peak areas.

tolerance of organic solvent was improved while its catalytic activity was similar to that of the wild-type enzyme.

To allow higher substrate concentrations, the kinetic resolution was examined in a buffer containing 10% (*v*/*v*) THF at 30 °C. Under these conditions, a threefold higher substrate concentration of *tert*-butyl-2-(2-bromopropanamido)acetate could be tested (5 mM, Table 4); THF can easily be removed from the reaction mixture after extraction of the substrates and products. Chiral HPLC showed that mutant G1 was active for more than 72 h and gave a substrate conversion of 53% under these conditions, whereas the wild-type enzyme was inactivated within 5 h and its substrate conversion was less than 3% (Table 4). The enzyme remained moderately enantioselective in this reaction (*E* value 28–30; 67 for wild type without co-solvent).[14c] This demonstrates that it was possible to enhance the solvent tolerance of the enzyme while retaining most of the catalytic properties. However, the organic co-solvent might reduce enantioselectivity. Although the amount of solubilized substrate could be increased both for β-HCH and *tert*-butyl 2-(2-bromopropanamido)acetate, the substrate-to-catalyst ratio remained rather low. To make this conversion more efficient, future enzyme engineering studies need to be performed to increase the enzymatic rates for these reactions.

Discussion

We describe here the use of a rapid computational design protocol for the stabilization of the LinB haloalkane dehalogenase. Most of the laboratory construction of libraries and thermostability screening (typical for directed-evolution projects) were replaced by in silico methods. Only 150 mutants were experimentally tested: 18 stabilizing mutations were found, as well as a combined variant that showed a 23 °C increase in apparent unfolding temperature and a more than 200-fold lower rate of inactivation. Less than 3% of the mutations that were analyzed in silico were examined experimentally. As computational screening is faster and cheaper than experimental screening, this FRESCO protocol[8f] provides an attractive route for rapid and cost-effective protein stabilization. Thermostabilization methods that rely on the experimental evaluation of large libraries of mutations usually require the screening of thousands of variants, as most random mutations are neutral

Table 4. Kinetic resolution of *tert*-butyl-2-(2-bromopropanamido)-acetate by wild-type LinB and G1 in the presence of 10% THF at 30 °C.

	Wild type				Mutant G1			
t [h]	*ee* substrate [%]	*ee* product [%]	Conversion [%]	*E*	*ee* substrate [%]	*ee* product [%]	Conversion [%]	*E*
0	0	<1	0		0		0	
5	2	<1	<3	–[a]	12	<1	<3	–[a]
24	0.3	<1	<3	–[a]	56	89	39	30
48	0.2	<1	<3	–[a]	80	84	49	28
72	0.6	<1	<3	–[a]	91	81	53	29

[a] Could not be calculated (low conversion).

or detrimental to stability,[2c] even when more advanced methods such as B-fitter[34] are used to identify target positions for mutagenesis. The FRESCO method, as demonstrated here for the stabilization of LinB and previously for limonene epoxide hydrolase,[8f] aims to eliminate mutations that do not contribute to the desired phenotype, by in silico methods instead of laboratory testing.

The increase in thermostability of the best LinB variant that carries three point mutations and a disulfide bond was accompanied by an increase in co-solvent tolerance. Similar correlations between thermostability and solvent tolerance were observed for haloalkane dehalogenase,[21] aminopeptidase,[33a] aldolase,[33b] ene-reductase,[33c] esterase,[6c] and other enzymes,[33d–g] thus suggesting a common biophysical mechanism. For example, the introduction of disulfide bonds, which in the case of LinB can prevent unfolding of the N terminus and reduce heat inactivation,[35] might also reduce unfolding in the presence of co-solvents, as, in both cases, the gain in entropy associated with (local) unfolding would be reduced. Polar solvents, such as DMSO, can inactivate enzymes by breaking hydrogen bonds and by removing or replacing essential water molecules in the solvent shell surrounding the protein.[33d,35] Apolar solvents, such as THF, can disrupt hydrophobic interactions in the protein interior; these are important for protein folding. There are several biophysical effects that can increase both thermo- and solvent stability, such as improvements to hydrophobic packing in the protein interior or the introduction of stabilizing interactions in flexible parts. The observed relationship between folding energy, thermostability, and solvent tolerance can be used to improve the co-solvent compatibility of enzymes more easily, as demonstrated here. The ability to improve enzyme stability in the presence of hydrophobic co-solvents (e.g., THF) can provide great benefits for downstream processing in biocatalytic conversion, such as facile product separation and recovery. Furthermore, solvent tolerance is often required for the use of hydrolytic enzymes in synthetic reactions,[36] and contributes to applicability in pharmaceutical synthesis[37] and polymer modification.[38]

Although the computational methods used in this work identified eighteen mutations that enhanced stability, a significant number of the mutations that were predicted to enhance stability appeared to lower LinB thermostability when tested experimentally. Incorrect predictions frequently involved the introduction of surface-exposed hydrophobic residues. These mutations can be discarded by visual inspection because they lack sufficient interaction with other hydrophobic groups. The energy calculations of FoldX and Rosetta favor introduction of such residues; this is (partially) in agreement with observations for small model proteins, where such mutations can be stabilizing.[10,11b] However, the introduction of hydrophobic side chains at the protein surface can be disadvantageous for the $T_{m,app}$ of larger proteins, which more easily aggregate.[22] A recent study by Jacak et al. showed that adaptations to the Rosetta energy function can prevent the formation of these hydrophobic patches on the protein surface; these can be applied in future computational enzyme stabilization.[22]

Partial unfolding of flexible areas of a protein can cause irreversible inactivation by aggregation.[13] Mutations that improve the stability of such areas might contribute to enhancing overall protein stability more than substitutions in less-flexible regions.[7b,27,31] The highly flexible regions that can serve as targets for stabilization can be detected by their high *B*-factors in crystal structures[39] or by high RMSF during MD simulations.[40] During the engineering of LinB, two strongly stabilizing point mutations ($\Delta T_{m,app} > 4$ °C) were discovered at residue 147, which is in a flexible helix (residues 138–150) that covers the active site (Table 1, Figure 1). Cα atoms in the loop between residues 138–150 are predicted to be relatively flexible, as was evident from the fivefold higher *B*-factors (compared to the average) and a 1.5-fold higher RMSF during an MD simulation. The latter is the highest RMSF of the whole protein (Figure 1C). Another prominent stabilizing mutation (A247F) is not itself in a flexible area, but has interactions with this flexible loop (Figures 1A and 2D). The only strongly stabilizing mutation found in a different region was a disulfide bond incorporated near the flexible N terminus of the protein. Therefore, it is likely that the most effective mutations enhance overall stability by reducing the unfolding of the weakest parts of the protein and thereby reduce protein inactivation rates (Figure 3C).

By identifying flexible regions where mutations affect stability, the sizes of libraries targeting enhanced stability can be significantly decreased.[6b] However, simply introducing the mutations at highly flexible residues (the B-fitter approach) might not always be the best option. For the stabilization of limonene epoxide hydrolase by FRESCO, the most effective point mutations were near flexible areas rather than in the flexible regions themselves.[8f] In LinB the mutations with the largest stabilizing effects were in flexible regions, but the majority of the moderately stabilizing mutations were not (Figure 1B); one highly stabilizing mutation was not in a flexible area but had interactions with it. These mutations would have been missed

if only highly flexible residues had been targeted for mutagenesis.

In many enzymes, the active site is one of the most flexible parts of the protein, and introducing stabilizing mutations into this region bears the risk of reducing enzymatic activity, as has been observed in studies on lysozyme,[41] barnase,[42] ribonuclease,[43] beta-lactamase,[44] protease,[45] enolase,[46] and citrate synthase.[47] However, other studies have shown that stabilizing mutations near the active site do not necessarily affect catalytic activity. Mutations at the entrance of the tunnel to the active site of haloalkane dehalogenase from *Rhodococcus rhodochrous* stabilized the enzyme but did not decrease catalytic activity;[21] similarly, the activity and stability of a lipase were improved concurrently.[48] The LinB active site is buried in the protein and can only be accessed after movements of the loops covering it.[49] Therefore, flexibility of these loops is important for substrate entrance or product release.[49b,50] We indeed observed a significant reduction in enzymatic activity of LinB by most stabilizing mutations introduced close to the active site. Four stabilizing mutations introduced at position D147 (Table 1, Figure 2C) caused a reduction in activity, likely due to stronger interactions between a flexible helix (residues 145–155) and a loop and helix covering the active site (residues 166–178 and 244–250); these increased stability but reduced activity with 1-bromopropane (Table 1).

The effect of stabilizing mutations on catalytic activity differed significantly depending on substrate (Tables 2 and 3) and the particular mutant enzyme. For variant G1 (no mutations near the active site), the conversion rates were nearly identical for 11 different substrates, even though the inactivation rate decreased 30-fold (Figure 3C) and $T_{m,app}$ and the catalytic activity at higher temperatures increased. However, with variant G3, three of the eleven substrates were converted ten times more slowly than with the wild-type enzyme, whereas the other eight substrates were converted only two to three times more slowly (or at a similar rate; Table 3).

In conclusion, the work reported here demonstrates that the thermostability and solvent tolerance of haloalkane dehalogenase can be simultaneously increased by using the FRESCO method for computational enzyme stabilization. Mutations introduced close to the active site were most stabilizing, but these should be chosen with care because they have a high probability of resulting in a loss of activity by influencing functional movement around the active site. By introducing mutations only at more distant positions, it was possible to engineer a variant that displayed both improved stability and fully preserved catalytic activity for all tested substrates. The increase in stability was accompanied by a large improvement in organic co-solvent tolerance, thus enhancing the biocatalytic potential of this enzyme.

Experimental Section

Computational design of stabilizing mutations by FRESCO: The FRESCO approach is based on the combined use of several computational algorithms to discover stabilizing mutations. To find stabilizing point mutations in LinB, all positions of the protein sequence were mutated in silico to all proteinogenic amino acids except cysteine. For each mutant, a 3D structure was predicted by FoldX[10] with the crystal structure of wild-type LinB[49a] as the template. The free energy difference between the folded and unfolded structures ($\Delta\Delta G^{fold}$) of these point mutants was predicted by both FoldX[10] and Rosetta,[11b] and was compared to that of wild type. $\Delta\Delta G^{fold}$ was used as a measure of enzyme stability. Settings described previously (Table 1, row 3 in ref. [11b]) were used for Rosetta calculations. For FoldX, the standard parameter settings, which have been tested on a large data set of point mutants, were used.[10]

The modeled three-dimensional structures of the mutants predicted to be stabilizing by FoldX or Rosetta were inspected visually in YASARA (http://www.yasara.org). Mutations that resulted in one of the following types of unfavorable interactions were excluded: 1) steric clashes, 2) internal cavities, 3) solvent-exposed aromatic residues, 4) solvent-exposed methionines,[51] 5) a hydrogen bond donor or acceptor that has fewer hydrogen bonding interactions than in wild type, 6) a large hydrophobic patch on the protein surface, 7) uncompensated removal of a salt bridge, and 8) destabilization of an α-helix by removal of α-helix capping.[52] In the field of computational design, visual inspection to eliminate designed variants with such defects is a standard step and is required because of insufficient conformational sampling and inaccuracies in the energy functions.[53] More details of this selection process are provided in the Supporting Information.

Mutations were treated in two categories for stability/activity investigations: those within 9 Å of any atom of the substrate (*tert*-butyl-2-(2-bromopropanamido)acetate), and those outside this area. To determine these distances, the substrate was modeled in the active site by using AutoDock 4.[54]

Positions suitable for the introduction of disulfide-bond forming cysteines were predicted by the Dynamic Disulfide Discovery (DDD) algorithm,[8f] for both the wild-type structure and snapshots of MD simulations for conformational sampling. Prediction of disulfide bonds is highly dependent on backbone conformation, and can be improved by the use of an ensemble of template structures generated by MD simulations. For the DDD procedure, the wild-type structure was placed in a water box and simulated at 298 K with the Yamber3 force field.[55] Five independent MD simulations were performed. For each simulation, the first 250 ps was used for equilibration, and after entering the production phase, snapshots were taken every 250 ps between 500 and 2500 ps, thus yielding 45 snapshots in total. From this ensemble of structures as a template, the DDD algorithm predicts disulfide bonds based on geometric constraints that are derived from the angles, dihedrals, and bond lengths of disulfide bonds in high-resolution structures in the protein database.[56] The structures of all predicted disulfide bonds were analyzed visually according to the screening criteria described in the previous section.

To eliminate mutations falsely predicted to be stabilizing, predicted point mutations and disulfide-bond mutants were screened by MD simulation. The simulations were based on the 3D structure of the mutant as predicted by FoldX, and used the Yamber3 force field.[55] Five 100 ps MD simulations were performed for each mutant. Each simulation started with a different random set of initial atom velocities, assigned according to a Maxwell–Boltzmann distribution. The temperature was increased from 5 to 298 K over 30 ps, followed by equilibration (20 ps) and production (50 ps). Snapshots were taken every 5 ps. For each variant, five independent MD simulations were performed. During each simulation, ten snapshots were recorded, and the average coordinates of these ten snapshots were calculat-

ed, to obtain one average structure per trajectory. If one of the trajectories displayed large local conformational differences compared to the other simulations, it was considered to be an outlier and was not used for further analysis. The resulting trajectories were visually screened by the criteria mentioned previously. Mutations were selected for experimental verification if they did not exhibit clearly unfavorable interactions during MD simulation.

Construction of mutants: A pBAD plasmid containing the *linB* gene from *Sphingomonas paucimobilis* UT26 (Uni*P*rot accession number P51698) attached to an N-terminal hexahistidine sequence was used throughout this study.[14c] Mutations to the *linB* gene were introduced by QuikChange mutagenesis (Agilent Technologies) with the PfuUltra Hotstart PCR Master Mix as recommended by the manufacturer. QuikChange PCR products were transformed into chemically competent *E. coli* TOP10 (Life Technologies). Incorporation of the mutations was confirmed by DNA sequencing. Successive rounds of mutagenesis were performed to construct variants containing multiple mutations. As *E. coli* often has difficulty with cytosolic production of proteins containing disulfide bonds, the production of variants containing these bonds was also performed in *E. coli* SHuffle (New England Biolabs). This strain is optimized for the production of cytosolic proteins containing disulfide bonds.[29]

Protein expression: Small-scale production (1.2 mL) of LinB was performed in deep-well microtiter plates (MTPs). Large-scale protein expression (1 L) was performed in terrific broth (TB: yeast extract (24 g L^{-1}), tryptone (12 g L^{-1}), glycerol (4 mL L^{-1}), KH_2PO_4 (17 mM), K_2HPO_4 (72 mM), pH 7.0). The medium was inoculated with 1% of an overnight culture and subsequently incubated at 37 °C with shaking at 200 rpm. At $OD_{600} = 0.6$ expression was induced by adding L-arabinose (0.02%, *w/v*) and the culture was grown for a further 16 h at 24 °C. Cells were harvested by centrifugation (2000 *g*, 15 min, 4 °C) and suspended in PN buffer (450 μL for small-scale experiments and 30 mL for large-scale experiments: potassium phosphate (50 mM, pH 7.5) with NaCl (150 mM)).

Small scale protein purification: Cells from a 1.2 mL culture were lysed by addition of FastBreak cell lysis reagent (50 μL, Promega) followed by incubation for 15 min at 30 °C with shaking at 200 rpm. To prepare cell-free extract, the lysate was centrifuged (2000 *g*, 45 min, 4 °C) and the supernatant was transferred to a clean MTP and used for protein purification. To purify proteins on a small scale, the MagneHis protein purification system (Promega) was used according to the manufacturer's instructions. Briefly, cell-free extract was incubated with magnetic beads suspension (10 μL), the beads were collected with a magnet, the supernatant was removed, and the beads were washed three times in PN buffer. LinB protein was eluted in elution buffer (200 μL; PN containing imidazole (500 mM)) and the magnetic beads were removed with the magnet. Subsequently, four rounds of dilution of the LinB solution in protein storage buffer (Na·HEPES (50 mM, pH 7.5)) and concentration in an Amicon Ultra-0.5 centrifugal filter (10 kDa cut-off, Merck Millipore) were performed to desalt the protein. The final enzyme solution (100 μL) was obtained with a protein concentration of ~0.2 mg mL^{-1}. SDS-PAGE showed that these samples contained >90% target protein.

Large-scale protein purification: The cells were lysed by sonication (10 s on, 30 s off, 10 min; 65 W, 20 kHz, 4 °C). Cell debris was removed by centrifugation (31 000 *g*, 45 min, 4 °C), then the supernatant was loaded on a Ni-NTA column (GE Healthcare) and washed with PN buffer (ten column volumes) and eluted by a linear gradient of elution buffer. Fractions that contained the desired protein were pooled and desalted into protein storage buffer by using a HiTrap desalting column (GE Healthcare). For all variants, the yield was 50 mg of protein per liter of culture. The sample was analyzed on a SDS-PAGE gel: a single band suggested that protein purity was >95%.

Enzyme assays: Catalytic activity by LinB variants was quantified by dehalogenation of the model substrate 1-bromopropane. Protein sample (20 μL, 0.2 mg mL^{-1} in protein storage buffer) was mixed with 1-bromopropane (285 μL, 30 mM in Tris·SO_4 (50 mM, pH 8.2)) in a microtiter plate. The mixture was incubated at 30 °C. Samples (40 μL) were removed at regular intervals and mixed with halide quantification reagent (160 μL; $NH_4Fe(SO_4)_2$ (16 μL, 0.25 M in HNO_3 (9 M)), saturated $Hg(SCN)_2$ (16 μL in ethanol), and deionized water (128 μL)). This reagent quenches the dehalogenation reaction and allows quantitative determination of halide concentration.[57] The samples were incubated for 5 min at 20 °C, and absorbance at 460 nm was measured with a Synergy Mx plate reader (BioTek, Winooski, VT). A calibration curve was made with NaBr, and the free bromide concentration was calculated. Where necessary, a calibration curve of free bromide in the presence of co-solvent was constructed to correct for the effect of co-solvent on the halide assay. A linear fit of this data was used to obtain the initial rate. Specific activities at different substrate concentrations were determined and fitted with the Michaelis–Menten equation to obtain kinetics parameters. Specific activities at higher temperatures were measured by incubating the protein sample for 5 min at the specified temperature and measuring specific activity at this temperature. A unit of catalytic activity (U) was defined as the conversion of 1 μmol of substrate in one minute.

The halide release assay was used to determine catalytic activities of dehalogenase variants with several chloro-, bromo-, and iodoalkanes, and halocycloalkanes. A linear calibration curve was used for bromide and iodine quantification; a polynomial calibration curve was used for chloride analysis. The substrate concentrations were chosen such that they were below the solubility limit of this compound in water and (if possible) above the reported K_m values for the dehalogenation reaction.[14a]

Protein concentrations were determined by absorbance at 280 nm ($\varepsilon_{280} = 5.6 \times 10^4$ M^{-1} cm^{-1}). For protein samples below 1.0 mL, concentration was determined with a NanoDrop 1000 spectrophotometer (Thermo Scientific).

Dehalogenation of β-HCH: β-HCH (2.88 mg; Sigma–Aldrich) was dissolved in DMSO (15 mL) to obtain a 660 μM solution. An aliquot (3.75 mL) of this was mixed in a 15 mL Pyrex tube with buffer (11.3 mL, potassium phosphate (50 mM, pH 7.5) with glycerol (10%)) and LinB (6.4 mg, 190 nmol; wild type or variant G1). The tube was incubated at 45 °C with shaking at 200 rpm, and samples (1 mL) were removed at regular intervals. β-HCH, pentachlorocyclohexanol, and tetrachlorocyclohexanediol were extracted with ethyl acetate (0.5 mL) containing 1,2,4-trichlorobenzene (4 μM; internal standard). This extract was dried with $MgSO_4$ and analyzed on a model 7890A gas chromatograph (Agilent) with an Rtx-1 column (Restek, Bellefonte, PA) and an electron capture detector, as described by Ito et al.[16] The baseline-separated signals of substrate β-HCH (retention time (t_R) 10.7 min) and products (tetrachlorocyclohexanediol ($t_R = 11.6$ min) and pentachlorocyclohexanol ($t_R = 11.8$ min)) were measured. To quantify substrate conversion, the peak area of β-HCH was divided by the peak area of the internal standard. This response value was converted to absolute concentration by using a calibration curve.

Kinetic resolution: The substrate *tert*-butyl-2-(2-bromopropanamido)-acetate was synthesized as reported by Westerbeek et al.[14c] To follow its kinetic resolution, *tert*-butyl-2-(2-bromopropanamido)-acetate (50 mM in THF) was diluted (1:10) in Tris·SO_4 (50 mM, pH 8.2) to obtain a 5 mM solution in a buffer/co-solvent mixture. An aliquot (15 mL) was incubated in a Pyrex tube in a water bath at 30 °C with wild-type LinB or LinB-G1 (0.5 mg mL^{-1}). Samples (1 mL) were removed at regular intervals, and the substrates and products were extracted with ethyl acetate (1 mL). This extract was dried with $MgSO_4$ and filtered. Volatiles were evaporated, and the enantiomeric excess of α-bromoamide and α-hydroxyamide was determined by chiral HPLC with an AD-H column (Chiralcel, Illkirch, France; 4.6×256 mm, 5 μm, heptane/*i*PrOH (95:5), flow rate 0.5 mL min^{-1}). Retention times for substrate: 22.4 (*R*) and 24.1 min (*S*); for product: 30.4 (*R*) and 36.1 min (*S*). The enantioselectivity (*E*) and conversions were calculated by substituting the measured enantiomeric excess of substrate and product into published equations.[58]

Determination of apparent melting temperatures: The thermofluor assay was used to determine $T_{m,app}$.[24] Sypro Orange (5 μL, 100-fold diluted; Life Technologies) was added to purified enzyme (20 μL, 0.2–1.5 mg mL^{-1}). This sample was transferred to a iQ PCR 96-well plate (Bio-rad, Hercules, CA) and sealed with iQ 96-well PCR Plate seal (Bio-rad). Fluorescence (RFU; λ_{ex} = 490 nm, λ_{em} = 575 nm) was monitored while the sample was heated from 20 to 99 °C (1.1 °C min^{-1}) in a CFX96 Q-PCR device (Bio-rad). $T_{m,app}$ was defined as the maximum of dRFU/d*T*. To determine $T_{m,app}$ after reduction of disulfide bonds, dithiothreitol (DTT, 10 mM) was added, and the mixture was incubated for 15 min at 20 °C before measurement.

Differential scanning calorimetry: Apparent melting temperatures were measured by DSC. Protein samples were dialyzed for 16 h against Na·HEPES (50 mM, pH 7.5) to remove salts. The $T_{m,app}$ was determined by measuring excess heat capacity of a protein sample (20 μM) while heating from 20 to 110 °C (1 °C min^{-1}) in a VP-DSC MicroCal system (GE Healthcare). A reference signal was measured with buffer in the same way and subtracted from the protein sample signal. The temperature at which the excess heat capacity was at a maximum was taken as $T_{m,app}$.

Thermal inactivation rates: Thermal inactivation rates were measured by incubating protein samples (0.2 mg mL^{-1} in protein storage buffer) for varying times at the specified temperatures, and subsequently incubating the enzymes at 4 °C for 5 min. The residual specific activity was then determined by using the standard activity assay. A plot of residual activity versus incubation time was fitted with a single exponential decay to obtain the irreversible thermal inactivation rate (k_{inact}). It was experimentally confirmed that the enzyme unfolded irreversibly by measuring the activity of thermally unfolded enzyme after incubating it at 4 °C for different time periods.

Acknowledgements

A.R.-S. was supported by a fellowship from Coordenação de Aperfeiçoamento de Pessoal de Nível Superior (CAPES/PDSE). We thank Malgorzata Murawska for help with obtaining chiral HPLC separations. This work was supported by the European Union 7th framework projects Metaexplore (KBBE-2007-3-3-05, 222625) and Kyrobio (KBBE-2011-5, 289646) and by NWO (Netherlands Organization for Scientific Research) through an ECHO grant.

Keywords: computational design · co-solvents · dehalogenases · directed evolution · thermostability · virtual screening

[1] U. T. Bornscheuer, G. W. Huisman, R. J. Kazlauskas, S. Lutz, J. C. Moore, K. Robins, *Nature* **2012**, *485*, 185 – 194.
[2] a) D. Böttcher, U. T. Bornscheuer, *Curr. Opin. Microbiol.* **2010**, *13*, 274 – 282; b) M. Goldsmith, D. S. Tawfik, *Curr. Opin. Struct. Biol.* **2012**, *22*, 406 – 412; c) N. Tokuriki, F. Stricher, L. Serrano, D. S. Tawfik, *PLoS Comput. Biol.* **2008**, *4*, e1000002.
[3] a) H. E. Schoemaker, D. Mink, M. G. Wubbolts, *Science* **2003**, *299*, 1694 – 1697; b) A. S. Bommarius, J. K. Blum, M. J. Abrahamson, *Curr. Opin. Chem. Biol.* **2011**, *15*, 194 – 200.
[4] a) O. Khersonsky, G. Kiss, D. Röthlisberger, O. Dym, S. Albeck, K. N. Houk, D. Baker, D. S. Tawfik, *Proc. Natl. Acad. Sci. USA* **2012**, *109*, 10358 – 10363; b) N. Tokuriki, D. S. Tawfik, *Curr. Opin. Struct. Biol.* **2009**, *19*, 596 – 604; c) J. D. Bloom, S. T. Labthavikul, C. R. Otey, F. H. Arnold, *Proc. Natl. Acad. Sci. USA* **2006**, *103*, 5869 – 5874; d) W. Besenmatter, P. Kast, D. Hilvert, *Proteins Struct. Funct. Bioinf.* **2007**, *66*, 500 – 506.
[5] a) V. G. H. Eijsink, S. Gåseidnes, T. V. Borchert, B. van den Burg, *Biomol. Eng.* **2005**, *22*, 21 – 30; b) M. Lehmann, L. Pasamontes, S. F. Lassen, M. Wyss, *Biochim. Biophys. Acta Protein Struct. Mol. Enzymol.* **2000**, *1543*, 408 – 415; c) B. van den Burg, V. G. H. Eijsink, *Curr. Opin. Biotechnol.* **2002**, *13*, 333 – 337; d) M. L. Rollence, D. Filpula, M. W. Pantoliano, P. N. Bryan, *Crit. Rev. Biotechnol.* **1988**, *8*, 217 – 224; e) F. H. Arnold, P. L. Wintrode, K. Miyazaki, A. Gershenson, *Trends Biochem. Sci.* **2001**, *26*, 100 – 106.
[6] a) J. K. Blum, M. D. Ricketts, A. S. Bommarius, *J. Biotechnol.* **2012**, *160*, 214 – 221; b) H. Jochens, D. Aerts, U. T. Bornscheuer, *Protein Eng. Des. Sel.* **2010**, *23*, 903 – 909; c) Y. Mei, N. Peng, S. Zhao, Y. Hu, H. Wang, Y. Liang, Q. She, *Appl. Microbiol. Biotechnol.* **2012**, *93*, 1965 – 1974; d) K. Watanabe, T. Ohkuri, S. Yokobori, A. Yamagishi, *J. Mol. Biol.* **2006**, *355*, 664 – 674.
[7] a) B. Van den Burg, G. Vriend, O. R. Veltman, G. Venema, V. G. H. Eijsink, *Proc. Natl. Acad. Sci. USA* **1998**, *95*, 2056 – 2060; b) V. G. H. Eijsink, A. Bjørk, S. Gåseidnes, R. Sirevåg, B. Synstad, B. van den Burg, G. Vriend, *J. Biotechnol.* **2004**, *113*, 105 – 120.
[8] a) J. E. Diaz, C.-S. Lin, K. Kunishiro, B. K. Feld, S. K. Avrantinis, J. Bronson, J. Greaves, J. G. Saven, G. A. Weiss, *Protein Sci.* **2011**, *20*, 1597 – 1606; b) B. Borgo, J. J. Havranek, *Proc. Natl. Acad. Sci. USA* **2012**, *109*, 1494 – 1499; c) H. J. Wijma, R. J. Floor, D. B. Janssen, *Curr. Opin. Struct. Biol.* **2013**, *23*, 588 – 594; d) X. Song, Y. Wang, Z. Shu, J. Hong, T. Li, L. Yao, *PLoS Comput. Biol.* **2013**, *9*, e1003129; e) B. Liu, J. Zhang, Z. Fang, L. Gu, X. Liao, G. Du, J. Chen, *J. Ind. Microbiol. Biotechnol.* **2013**, *40*, 697 – 704; f) H. J. Wijma, R. J. Floor, P. A. Jekel, D. Baker, S. J. Marrink, D. B. Janssen, *Protein Eng. Des. Sel.* **2014**, *27*, 49 – 58.
[9] A. V. Gribenko, M. M. Patel, J. Liu, S. A. McCallum, C. Wang, G. I. Makhatadze, *Proc. Natl. Acad. Sci. USA* **2009**, *106*, 2601 – 2606.
[10] R. Guerois, J. E. Nielsen, L. Serrano, *J. Mol. Biol.* **2002**, *320*, 369 – 387.
[11] a) A. B. Daugherty, P. Muthu, S. Lutz, *Biochemistry* **2012**, *51*, 8247 – 8255; b) E. H. Kellogg, A. Leaver-Fay, D. Baker, *Proteins Struct. Funct. Bioinf.* **2011**, *79*, 830 – 838.
[12] a) X.-W. Yu, N.-J. Tan, R. Xiao, Y. Xu, *PLoS One* **2012**, *7*, e46388; b) Z.-l. Han, S.-y. Han, S.-p. Zheng, Y. Lin, *Appl. Microbiol. Biotechnol.* **2009**, *85*, 117 – 126; c) A. A. Dombkowski, *Bioinformatics* **2003**, *19*, 1852 – 1853; d) C. R. Robinson, R. T. Sauer, *Biochemistry* **2000**, *39*, 12494 – 12502.
[13] a) V. Potapov, M. Cohen, G. Schreiber, *Protein Eng. Des. Sel.* **2009**, *22*, 553 – 560; b) G. Thiltgen, R. A. Goldstein, *PLoS One* **2012**, *7*, e46084.
[14] a) J. Kmunícek, K. Hynková, T. Jedlicka, Y. Nagata, A. Negri, F. Gago, R. C. Wade, J. Damborský, *Biochemistry* **2005**, *44*, 3390 – 3401; b) Y. Nagata, K. Miyauchi, J. Damborsky, K. Manova, A. Ansorgova, M. Takagi, *Appl. Environ. Microbiol.* **1997**, *63*, 3707 – 3710; c) A. Westerbeek, W. Szymański, H. J. Wijma, S. J. Marrink, B. L. Feringa, D. B. Janssen, *Adv. Synth. Catal.* **2011**, *353*, 931 – 944; d) A. Westerbeek, J. G. E. van Leeuwen, W. Szymański, B. L. Feringa, D. B. Janssen, *Tetrahedron* **2012**, *68*, 7645 – 7650; e) W. Szymański, A. Westerbeek, D. B. Janssen, B. L. Feringa, *Angew. Chem. Int. Ed.* **2011**, *50*, 10712 – 10715; *Angew. Chem.* **2011**, *123*, 10900 – 10903.
[15] Y. Nagata, T. Nariya, R. Ohtomo, M. Fukuda, K. Yano, M. Takagi, *J. Bacteriol.* **1993**, *175*, 6403 – 6410.

[16] M. Ito, Z. Prokop, M. Klvana, Y. Otsubo, M. Tsuda, J. Damborsky, Y. Nagata, *Arch. Microbiol.* **2007**, *188*, 313 – 325.
[17] a) M. Monincová, Z. Prokop, J. Vévodová, Y. Nagata, J. Damborský, *Appl. Environ. Microbiol.* **2007**, *73*, 2005 – 2008; b) V. A. Streltsov, Z. Prokop, J. Damborský, Y. Nagata, A. Oakley, M. C. J. Wilce, *Biochemistry* **2003**, *42*, 10104 – 10112; c) J. Marek, J. Vévodová, I. K. Smatanová, Y. Nagata, L. A. Svensson, J. Newman, M. Takagi, J. Damborský, *Biochemistry* **2000**, *39*, 14082 – 14086.
[18] L. Biedermannová, Z. Prokop, A. Gora, E. Chovancová, M. Kovács, J. Damborský, R. C. Wade, *J. Biol. Chem.* **2012**, *287*, 29062 – 29074.
[19] M. Boháč, Y. Nagata, Z. Prokop, M. Prokop, M. Monincová, M. Tsuda, J. Koča, J. Damborský, *Biochemistry* **2002**, *41*, 14272 – 14280.
[20] V. Stepankova, J. Damborsky, R. Chaloupkova, *Biotechnol. J.* **2013**, *8*, 719 – 729.
[21] T. Koudelakova, R. Chaloupkova, J. Brezovsky, Z. Prokop, E. Sebestova, M. Hesseler, M. Khabiri, M. Plevaka, D. Kulik, I. Kuta Smatanova, P. Rezacova, R. Ettrich, U. T. Bornscheuer, J. Damborsky, *Angew. Chem. Int. Ed.* **2013**, *52*, 1959 – 1963; *Angew. Chem.* **2013**, *125*, 2013 – 2017.
[22] R. Jacak, A. Leaver-Fay, B. Kuhlman, *Proteins Struct. Funct. Bioinf.* **2012**, *80*, 825 – 838.
[23] a) L. S. D. Caves, J. D. Evanseck, M. Karplus, *Protein Sci.* **1998**, *7*, 649 – 666; b) S. Genheden, U. Ryde, *J. Comput. Chem.* **2011**, *32*, 187 – 195.
[24] U. B. Ericsson, B. M. Hallberg, G. T. DeTitta, N. Dekker, P. Nordlund, *Anal. Biochem.* **2006**, *357*, 289 – 298.
[25] a) W. J. Becktel, J. A. Schellman, *Biopolymers* **1987**, *26*, 1859 – 1877; b) S. Robic, *CBE Life Sci. Educ.* **2010**, *9*, 189 – 195.
[26] W. Augustyniak, A. A. Brzezinska, T. Pijning, H. Wienk, R. Boelens, B. W. Dijkstra, M. T. Reetz, *Protein Sci.* **2012**, *21*, 487 – 497.
[27] a) G. Vriend, V. Eijsink, *J. Comput.-Aided Mol. Des.* **1993**, *7*, 367 – 396; b) Y. Ding, Y. Cai, *Biopolymers* **2013**, *99*, 594 – 604.
[28] J. G. E. van Leeuwen, H. J. Wijma, R. J. Floor, J.-M. van der Laan, D. B. Janssen, *ChemBioChem* **2012**, *13*, 137 – 148.
[29] J. Lobstein, C. Emrich, C. Jeans, M. Faulkner, P. Riggs, M. Berkmen, *Microb. Cell Fact.* **2012**, *11*, 56.
[30] B. S. Melnik, T. V. Povarnitsyna, A. S. Glukhov, T. N. Melnik, V. N. Uversky, R. H. Sarma, *J. Biomol. Struct. Dyn.* **2012**, *29*, 815 – 824.
[31] N. C. Benson, V. Daggett, *Protein Sci.* **2008**, *17*, 2038 – 2050.
[32] M. Otyepka, J. Damborský, *Protein Sci.* **2002**, *11*, 1206 – 1217.
[33] a) A. R. Khan, S. Nirasawa, S. Kaneko, T. Shimonishi, K. Hayashi, *Enzyme Microb. Technol.* **2000**, *27*, 83 – 88; b) J. Hao, A. Berry, *Protein Eng. Des. Sel.* **2004**, *17*, 689 – 697; c) S. Reich, N. Kress, B. M. Nestl, B. Hauer, *J. Struct. Biol.* **2014**, *185*, 228 – 233; d) N. Doukyu, H. Ogino, *Biochem. Eng. J.* **2010**, *48*, 270 – 282; e) P. V. Iyer, L. Ananthanarayan, *Process Biochem.* **2008**, *43*, 1019 – 1032; f) H. Ogino, H. Ishikawa, *J. Biosci. Bioeng.* **2001**, *91*, 109 – 116; g) G. A. Sellek, J. B. Chaudhuri, *Enzyme Microb. Technol.* **1999**, *25*, 471 – 482.
[34] a) M. T. Reetz, P. Soni, L. Fernández, Y. Gumulya, J. D. Carballeira, *Chem Commun.* **2010**, *46*, 8657 – 8658; b) M. T. Reetz, J. D. Carballeira, A. Vogel, *Angew. Chem. Int. Ed.* **2006**, *45*, 7745 – 7751; *Angew. Chem.* **2006**, *118*, 7909 – 7915.
[35] V. A. Sirotkin, *Biochim. Biophys. Acta Proteins Proteomics* **2005**, *1750*, 17 – 29.
[36] a) H.-C. Jung, S.-J. Kwon, J.-G. Pan, *BMC Biotechnol.* **2006**, *6*, 23; b) Y.-M. Kim, D. Kim, A. Kimura, *Biotechnol. Bioprocess Eng.* **2008**, *13*, 639 – 645.
[37] C. K. Savile, J. M. Janey, E. C. Mundorff, J. C. Moore, S. Tam, W. R. Jarvis, J. C. Colbeck, A. Krebber, F. J. Fleitz, J. Brands, P. N. Devine, G. W. Huisman, G. J. Hughes, *Science* **2010**, *329*, 305 – 309.
[38] A. W. P. Jarvie, N. Overton, C. B. St Pourçain, *Perkin Trans. 1* **1999**, 2171 – 2176.
[39] P. Radivojac, Z. Obradovic, D. K. Smith, G. Zhu, S. Vucetic, C. J. Brown, J. D. Lawson, A. K. Dunker, *Protein Sci.* **2004**, *13*, 71 – 80.
[40] M. G. Pikkemaat, A. B. M. Linssen, H. J. C. Berendsen, D. B. Janssen, *Protein Eng.* **2002**, *15*, 185 – 192.
[41] B. K. Shoichet, W. A. Baase, R. Kuroki, B. W. Matthews, *Proc. Natl. Acad. Sci. USA* **1995**, *92*, 452 – 456.
[42] E. M. Meiering, L. Serrano, A. R. Fersht, *J. Mol. Biol.* **1992**, *225*, 585 – 589.
[43] A. Mukaiyama, M. Haruki, M. Ota, Y. Koga, K. Takano, S. Kanaya, *Biochemistry* **2006**, *45*, 12673 – 12679.
[44] B. M. Beadle, B. K. Shoichet, *J. Mol. Biol.* **2002**, *321*, 285 – 296.
[45] S. Kidokoro, Y. Miki, K. Endo, A. Wada, H. Nagao, T. Miyake, A. Aoyama, T. Yoneya, K. Kai, S. Ooe, *FEBS Lett.* **1995**, *367*, 73 – 76.
[46] R. A. Nagatani, A. Gonzalez, B. K. Shoichet, L. S. Brinen, P. C. Babbitt, *Biochemistry* **2007**, *46*, 6688 – 6695.
[47] W. Zhi, P. A. Srere, C. T. Evans, *Biochemistry* **1991**, *30*, 9281 – 9286.
[48] M. Z. Kamal, T. A. S. Mohammad, G. Krishnamoorthy, N. M. Rao, *PLoS One* **2012**, *7*, e35188.
[49] a) A. J. Oakley, M. Klvaňa, M. Otyepka, Y. Nagata, M. C. J. Wilce, J. Damborský, *Biochemistry* **2004**, *43*, 870 – 878; b) M. Okai, J. Ohtsuka, L. F. Imai, T. Mase, R. Moriuchi, M. Tsuda, K. Nagata, Y. Nagata, M. Tanokura, *J. Bacteriol.* **2013**, *195*, 2642 – 2651.
[50] Z. Prokop, M. Monincová, R. Chaloupková, M. Klvaňa, Y. Nagata, D. B. Janssen, J. Damborský, *J. Biol. Chem.* **2003**, *278*, 45094 – 45100.
[51] B. C. Lee, A. Dikiy, H.-Y. Kim, V. N. Gladyshev, *Biochim. Biophys. Acta Gen. Subj.* **2009**, *1790*, 1471 – 1477.
[52] D. E. Blagdon, M. Goodman, *Biopolymers* **1975**, *14*, 241 – 245.
[53] a) U. Y. Ulge, D. A. Baker, R. J. Monnat, Jr., *Nucleic Acids Res.* **2011**, *39*, 4330 – 4339; b) G. Kiss, N. Çelebi-Ölçüm, R. Moretti, D. Baker, K. N. Houk, *Angew. Chem. Int. Ed.* **2013**, *52*, 5700 – 5725; *Angew. Chem.* **2013**, *125*, 5810 – 5836; c) H. J. Wijma, D. B. Janssen, *FEBS J.* **2013**, *280*, 2948 – 2960.
[54] G. M. Morris, R. Huey, W. Lindstrom, M. F. Sanner, R. K. Belew, D. S. Goodsell, A. J. Olson, *J. Comput. Chem.* **2009**, *30*, 2785 – 2791.
[55] E. Krieger, T. Darden, S. B. Nabuurs, A. Finkelstein, G. Vriend, *Proteins Struct. Funct. Bioinf.* **2004**, *57*, 678 – 683.
[56] M. T. N. Petersen, P. H. Jonson, S. B. Petersen, *Protein Eng.* **1999**, *12*, 535 – 548.
[57] I. Iwasaki, S. Utsumi, T. Ozawa, *Bull. Chem. Soc. Jpn.* **1952**, *25*, 226 – 226.
[58] C. S. Chen, Y. Fujimoto, G. Girdaukas, C. J. Sih, *J. Am. Chem. Soc.* **1982**, *104*, 7294 – 7299.

Received: March 26, 2014
Published online on June 27, 2014